Ecological Applications, 26(4), 2016, pp. 1125–1135

Estimating population density and connectivity of American mink using spatial capture–recapture

Angela K. Fuller,[1,6] Chris S. Sutherland,[2,5] J. Andrew Royle,[3] and Matthew P. Hare[4]

[1]*U.S. Geological Survey, New York Cooperative Fish and Wildlife Research Unit, Department of Natural Resources, Cornell University, 211 Fernow Hall, Ithaca, New York 14853 USA*
[2]*New York Cooperative Fish and Wildlife Research Unit, Department of Natural Resources, Cornell University, Bruckner Hall, Ithaca, New York 14853 USA*
[3]*U.S. Geological Survey, Patuxent Wildlife Research Center, Laurel, Maryland 20708 USA*
[4]*Department of Natural Resources, Cornell University, 205 Fernow Hall, Ithaca, New York 14853 USA*

Abstract. Estimating the abundance or density of populations is fundamental to the conservation and management of species, and as landscapes become more fragmented, maintaining landscape connectivity has become one of the most important challenges for biodiversity conservation. Yet these two issues have never been formally integrated together in a model that simultaneously models abundance while accounting for connectivity of a landscape. We demonstrate an application of using capture–recapture to develop a model of animal density using a least-cost path model for individual encounter probability that accounts for non-Euclidean connectivity in a highly structured network. We utilized scat detection dogs (*Canis lupus familiaris*) as a means of collecting non-invasive genetic samples of American mink (*Neovison vison*) individuals and used spatial capture–recapture models (SCR) to gain inferences about mink population density and connectivity. Density of mink was not constant across the landscape, but rather increased with increasing distance from city, town, or village centers, and mink activity was associated with water. The SCR model allowed us to estimate the density and spatial distribution of individuals across a 388 km^2 area. The model was used to investigate patterns of space usage and to evaluate covariate effects on encounter probabilities, including differences between sexes. This study provides an application of capture–recapture models based on ecological distance, allowing us to directly estimate landscape connectivity. This approach should be widely applicable to provide simultaneous direct estimates of density, space usage, and landscape connectivity for many species.

Key words: abundance; American mink; animal movement; connectivity; density; non-invasive genetics; scat detection dog; spatial capture–recapture.

Introduction

Estimating the abundance or density of animal populations is fundamental to the conservation and management of wild living populations (Williams et al. 2002), providing insights into species ecological relationships. Often the objective is simply to estimate the density of a population, but learning how individuals are distributed throughout space as a function of resources or covariates of interest can have broader relevance to conservation and management. Further, as landscapes become more fragmented, there is increasing interest in maintaining landscape connectivity for animals, with much recent focus on developing models describing landscape resistance to movement (for a review see Zeller et al. 2012). Spatial capture–recapture (SCR) models are becoming widely used to model density of animal populations using field methods that generate spatially explicit individual encounter histories and have recently been used to investigate ecological processes such as resource selection (Royle et al. 2013*b*) and landscape connectivity (Royle et al. 2013*a*, Sutherland et al. 2015). General models of animal movement are typically based on Euclidean distance, despite studies that suggest that movement can be influenced by the spatial configuration of habitat or landscape structure (Fagan 2002, Grant et al. 2009). Spatial capture–recapture models in which encounter probability is based on distance measured as related to hypotheses of how animals move through the landscape (i.e., ecological distance) have not yet been applied in practice. Instead, all applications of SCR to date have assumed that animals distribute their activity in certain ways, which is often bivariate normal and based on the Euclidean distance between an activity center and a trap, which ignores the effects of landscape structure on animal movement.

Manuscript received 24 February 2015; revised 27 August 2015; accepted 16 September 2015; final version received 23 October 2015. Corresponding Editor: T. O'Brien.

[5]Present address: Department of Environmental Conservation, University of Massachusetts-Amherst, 118 Holdsworth Hall Amherst, MA 01003-9285

[6]E-mail: angela.fuller@cornell.edu

In this paper, we demonstrate the first application of an SCR model (Sutherland et al. 2015) that uses an ecological-distance based encounter probability model, incorporating and evaluating the effects of landscape covariates on both the spatial distribution of density and space use within an individual's home range. We apply this class of SCR models to a population of American mink (*Neovison vison*), a semi-aquatic carnivorous mustelid native to North America, which serve as economically important furbearers and top predators in aquatic systems across most of their native range (Dunstone 1993). Mink play an important role as sentinel species in environmental health (Basu et al. 2007), but despite the importance of mink, the few studies in North America have focused on describing general habitat preferences without direct links to density (Marshall 1936, Burgess and Bider 1980, Racey and Euler 1983, Loukmas and Halbrook 2001, Wolff et al. 2015). Further, population estimates of mink in North America typically rely on harvest data (Erb et al. 2001, Haydon et al. 2001, Shier and Boyce 2009), which can be biased by the act of trapping and trapper behavior. Additionally, American mink are riparian habitat specialists and the fact that they are more likely to move along, rather than away from, water suggests that such behavior may violate the Euclidean distance assumption. Sutherland et al. (2015) demonstrated that violations of the Euclidean distance assumptions can bias estimates of density and suggest that the ecological distance model based on least-cost path (Beier et al. 2008, Royle et al. 2013*a*) is a preferable model for the encounter process in highly structured landscapes, such as stream networks, which occur as highly branched and connected paths. The application of SCR to mink provides an opportunity to evaluate the utility of these models within a highly structured landscape, providing unique challenges in the collection of encounter history data from a species that occurs at low densities and is elusive.

The objective of our study was to develop spatial models of mink density that account for the connectivity of the landscape in the form of non-Euclidean structure of stream networks used by the species. We use spatial capture–recapture models with newly developed least-cost path distance models (Royle et al. 2013*a*, Sutherland et al. 2015) to describe encounter probability of individual mink, and non-invasive genetic sampling from scat obtained by sampling space with detector dogs. We compare estimates obtained by standard Euclidean distance models and models based on least-cost path distance.

Materials and Methods

Study design and mink scat collection

Our 388-km^2 study area is centered on a 26-km stretch of the Mohawk River, 42°58′ 5.6316″N, 74°38′33.5688″W, including all tributaries off the main stem of the river (Fig. 1). We centered transects on road-stream intersections which reduced time spent traveling to and from sites and maximized the number of sites visited in the sampling window from 1 to 17 July 2012. This short sampling window minimized potential effects of variable weather and temperature on scat decay rates and effectiveness of scat detection dogs. The sampling period also represents a time period that is demographically closed (i.e., no recruitment and no mortality related to the trapping season that occurs during winter), occurring after the breeding season (Enders 1952) and prior to juvenile dispersal (Niemimma 1955, Gerell 1970, Dunstone 1993).

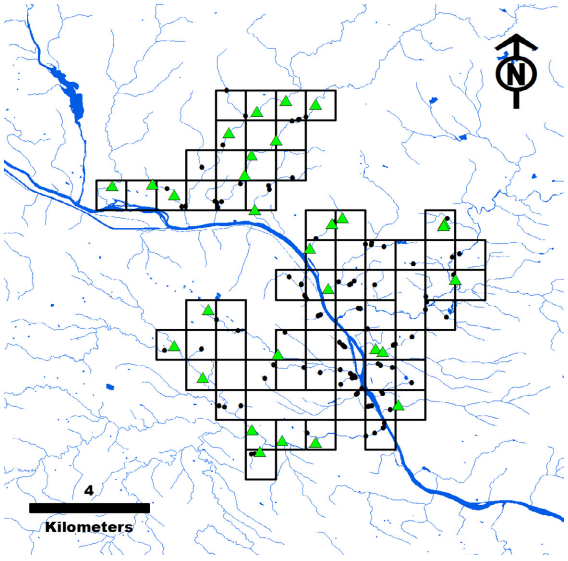

Fig. 1. The Mohawk study area depicting all potential sites (black points, n = 105) and surveyed sites (green triangles, n = 28), within an interior sampling grid of 1 km^2 cells (n = 58).

We devised a grid-based sampling design based on trying to achieve an average spacing of sites between 1 and 2 times the σ parameter of the half-normal SCR model, slightly closer than the optimal suggestions of Sollmann et al. (2012), but meant to safeguard against too few spatial recaptures and achieve sampling efficiency. Home range size of mink estimated from our study area was 1 km^2 (unpublished data), therefore we divided the study area into 1-km^2 grid cells and attempted to sample one site per grid cell. Within the central portion of the study area there were 105 potential stream/road intersections within 58 grid cells (Fig. 1). We proceeded with site selection as follows: if the cell had more than one site, we attempted to gain landowner permission to access the most central site. If permission was denied for that site, we then sought landowner permission for the next most central site. If permission was denied for all sites within the targeted cell, we chose a new cell that was contiguous to a cell that was already identified as a viable cell (i.e., landowner permission had already been obtained).

We surveyed 28 stream transects within twenty-eight 1-km^2 grid cells ($\bar{X} \pm$SD distance between survey sites

was 1.1 km ± 535 m), with each transect surveyed once during the sampling window. Transects varied in length according to whether or not permission was granted to access continuous stream sections (mean = 1.05 km; range, 0.18 km and 3.72 km). We used a single scat detection dog (Australian cattle dog) trained to locate mink scat by scent. The dog was professionally trained by Conservation Canines (University of Washington, Center for Conservation Biology, Seattle, Washington, D.C., USA) using 17 mink scats collected from multiple locations within the study area, representing nine genetically identified unique individuals that could potentially have different diets. Dogs were trained to sit when they located a scat and this behavior resulted in the dog receiving a reward (i.e., a ball). The dog was acclimated to the area and 1 week of on-site training was conducted by visiting sites where we had previously detected confirmed mink scats, as well as training the dogs on previously frozen mink scats that were placed on stream banks. These training areas were not visited during subsequent surveys in the study.

The dog team consisted of the detection dog, a dog handler, and an orienteer who processed samples that were collected. We used the same dog and dog handler for the duration of the study. The dog searched off-leash, allowing the dog to move according to wind direction and associated scent cues. Sampling was conducted in the morning to maximize moisture and air movement and to minimize heat stress to the dog; the dog worked <6 h/d. The handler worked the dog to search a transect ≤10 m from the river/stream edge (Bonesi and Macdonald 2004). This distance of the handler/dog from the river edge was deemed optimal given that Yamaguchi et al. (2003) reported that female and male mink stayed within 10 m of the nearest water source, 95% and 88% of the time, respectively. Further, Reed et al. (2011) reported that dogs detected >75% of scats located within 10 m with a decrease in the dogs' detection rates with increasing distance of scats from the transect line. Sampling along river/stream edges within a stream network setting allowed us to sample streams that are close in Euclidean space, and if the spatial pattern of observations deviates from Euclidean-based expectations, allows us to calculate a parameter associated with apparent costs associated with landscape structure (see Section Materials and Methods: Spatial capture–recapture model and Fig. 2 for further explanation). When scat was found, the exact location was recorded with a handheld GPS (Garmin GPSMAP 60CSX, Lenexa, Kansas, USA). Scat samples were collected and stored in waxless paper bags and were air dried for ≥24 h before being preserved in Falcon tubes (Falcon® tubes, VWR, Radnor, Pennsylvania, USA) with 96% ethanol.

To construct spatially explicit encounter histories, each site consisted of one transect that was divided into 25-m sections which were regarded as effective traps (trap from here on) in the development of SCR models, and scat encounters were associated with 25 m stream sections. The choice of 25-m was to ensure that the effective trap size was small enough relative to the home range size of mink to allow for detections in multiple traps, but also large enough for computational tractability relative to a continuous space model. We then constructed individual trap-specific binary encounter histories based on the genetic identification of individual mink (see Appendix S1).

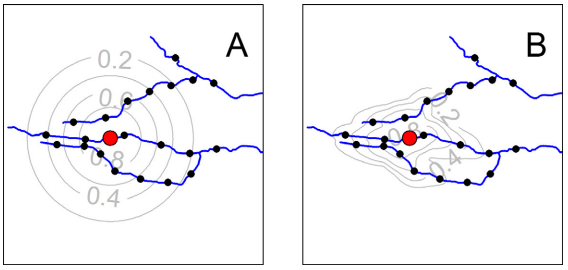

FIG. 2. Here we illustrate how the cost parameter α_2 can be estimated when sampling occurs only on the water course in a stream network setting. Under a given model, there is an expected capture probability that is a function of distance. Sampling streams sections that are close in Euclidean space generates a spatial pattern of observations that, if it deviates from Euclidean-based expectations, provides information about apparent costs associated with the landscape structure of interest. Here the stream network is shown in blue, a hypothetical activity center is shown as the larger red point, while the smaller black points represent sampling locations. (A) shows the contours of relative space-use under a Euclidean-distance based model ($\alpha_2 = 0$). (B) shows the contours of the relative space-use when there is an association between space use and landscape structure (in this case the use of space away from the water course is less frequent, i.e., $\alpha_2 > 0$). Comparing the two contour plots shows that expected patterns of observations differ, providing a mechanism to estimate α_2 when sampling different stream sections occurs close enough in space relative to scale of movement.

Genetic analyses

We extracted DNA using the QIAamp (Qiagen, Valencia, California, USA) stool extraction protocol for human DNA. Polymerase chain reaction (PCR) was used to amplify 14 loci using previously published mink-specific microsatellite and sexing markers. Two microsatellite loci had higher error rates and missing data, so 12 loci were analyzed (See Appendix S1: Table S1). The sexing marker, ZFX/ZFY, was amplified according to Shimatani et al. (2010) and the results visualized with ethidium bromide in 1.5% agarose gels alongside a 100 base-pair size ladder (Invitrogen, Carlsbad, California, USA). Unambiguous ZFX/ZFY results were accepted without replication, or retested up to three times to resolve disagreements with majority rule. Sex was scored as missing if disagreements were unresolvable.

A portion of the mitochondrial cytochrome oxidase I (COI) gene was amplified and Sanger sequenced from both strands to confirm species identification. All specimens were initially screened using four microsatellite loci (Mvi1321, Mvi1016, Mer095, Mer022) co-loaded for fragment analysis and those missing data for three

or more loci were dropped (i.e., they had insufficient DNA quality/quantity for further analysis). For the remainder, two PCR replicates were performed for each locus and additional replication up to six times followed only for genotypes of marginal quality, if initial replicates did not agree, or if the specimen ended up mismatching another specimen by only one to two alleles (out of 24). A consensus genotype across replicates was assembled by requiring only one observation of an alternate allele to score a heterozygous genotype. This scoring procedure was based on a consistent asymmetry observed between allelic dropout and false allele error rates across 13 noninvasive genotyping studies reviewed by Lampa et al. (2013), all using scat. Genotypes were recorded as missing if a locus yielded less than two positive PCR amplicons, if DNA was exhausted before ambiguities were resolved, or when a specimen yielded greater than two alleles across replicates. After deducing consensus genotypes, we disregarded any specimen missing genotypes at more than six of 12 microsatellite loci. Genotyping error rates were calculated on a per locus, per replicate basis only from the first two replicates because these were performed without regard for genotype quality (as in Ruibal et al. 2009). Two methods were used to estimate genotyping error. The genotypic mismatch rate per replicate was measured as the number of genotypic mismatches (in the first two replicates) from the consensus, divided by the total number of successfully replicated specimens times two (two replicates). Second, allele dropout per replicated heterozygote and false allele rate per replicate were estimated from the first two replicates as described by Pompanon et al. (2005). We used conservative matrix groupings (see Appendix S1) as a starting point to conduct likelihood ratio tests to evaluate and rank the probability of genotype matches (true recaptures) in pairwise contrasts after accounting for genotyping mismatch rate, as implemented in SHAZA 2.01 (Macbeth et al. 2011).

The probability of identity (PID) measures the theoretical likelihood of two multilocus genotypes being identical by chance if drawn from a Hardy–Weinberg equilibrium population, assuming independent loci. Mistakenly interpreting two unique individuals as identical (type I error) is avoided with low PID marker panels. The magnitude of PID depends on the number of loci, the number of alleles per locus, and the relatedness of individuals within the population (Waits et al. 2001). We used allele frequencies estimated from the final inferred set of individuals (see Results: Genetic results) to calculate heterozygosity and theoretical PID using Gimlet 1.3.3 (Valière 2002). We calculated unbiased PID for unrelated individuals as a lower bound and PID for siblings (PID(sib)) as an upper bound. The probability of randomly drawing an observed genotype from the population was calculated with Gimlet (mismatch probability). Hardy–Weinberg was tested using Genepop 4.2 (Rousset 2008).

Spatial capture–recapture model

A standard spatial capture–recapture (SCR) analysis requires spatial encounter histories y_{ijk} that denote the detection (or not) of $i = 1,\ldots, n$ individuals detected in $j = 1,\ldots, J$ traps on $k = 1, \ldots, K$, occasions. Each transect was surveyed once (i.e., $K = 1$) and discretization of the stream transects resulted in $j = 599$ effective traps with geographic coordinates $x_j = \{x_{1j}, x_{2j}\}$. Spatial encounter histories were reconstructed from the genetic analyses (see Results: Genetic results). For the basic SCR model under binomial sampling, encounter frequencies y_{ijk} are assumed to be Bernoulli random variables such that

$$y_{ijk} \sim \text{Bernoulli}(p_{ij}).$$

The probability of detecting individual i in trap j is p_{ij} and is modeled using an encounter model proportional to a Gaussian probability density function

$$p_{ij} = p_0 \times e^{-\alpha_{1,\text{sex}} d(x_j, s_i)^2}, \quad (1)$$

where $\alpha_{1,sex} = 1/\left(2\sigma^2_{\text{sex}}\right)$ and $d(x_j, s_i)$ is the Euclidean distance between an individuals activity center s_i and trap location x_j. Here, σ^2 (and therefore α_1) is indexed by sex, which allows for sex-specific differences in the spatial scale of space use to be investigated. We treat sex as a random variable in the model having a Bernoulli distribution with parameter probability of being a male that is estimated from the data. This model component allows for the handling of missing sex information (i.e., when the sex marker did not amplify; see Royle et al. 2015 for the model describing missing covariate values for sex). Parameter p_0 is the baseline encounter probability, which can also vary by sex. Although many other functions for encounter probability are possible, there is no biological basis for choosing among them as they do not correspond to explicit biological hypotheses and, as such, we did not consider alternative encounter probability models, although we do consider alternative, biologically motivated, models of distance (i.e., Euclidean vs. ecological distance).

In addition to modeling encounter probability as a function of the distance between activity centers and traps (Eq. 1), SCR models allow the parameter p_0 to be modeled as a function of any number of trap level covariates, **P**, that are thought to influence encounter probabilities as follows:

$$\text{logit}\left(p_{0,ij}\right) = \beta_{0,sex} + \beta_1 P_{1j} + \ldots + \beta_m P_{mj}.$$

We expected the probability of encounter to decline as the percent vegetative cover increases because it could become more difficult for dogs to locate scats in dense vegetation. Therefore, we investigated the influence of percentage of overstory and understory vegetation (deciduous, coniferous, and mixedwood trees >5 m tall and >20% vegetative cover, and shrubs and trees <5 m tall, including shrubs and young trees in an early successional

stage) on encounter probability (P_{cover}). P_{cover} was calculated using the 2006 National Landcover Database (NLCD; 30 × 30 m resolution) by summarizing the percent overstory and understory vegetation for each trap within a 25 × 25 m grid cell centered on each trap (see Materials and Methods: Study design and mink scat collection).

In the encounter model of Eq. 1 the trap locations x_j are known, but the activity centers s_i are latent variables. SCR models regard the activity centers as a realization of a point process having state space (possible outcomes) $\mathcal{S}$. For computational expediency, $\mathcal{S}$ was defined by the center points of regularly spaced 200 × 200 m grid cells (n = 9702) within a ~4 km buffer around the outermost traps in the north-south, east-west direction with a total area of 388 km^2. The use of 4 km was chosen to ensure that $\mathcal{S}$ represented a "subset of the plane that contains plausible animal locations" (Efford et al. 2009) and was three times the size of the expected scale parameter σ for males. The choice of 200 × 200 m grid cells represents a trade-off between being coarse enough for computational tractability and fine enough to provide information about the scatting behavior of mink (i.e., the opportunity for multiple activity centers to occur in the region of the trap within the effective trapping area). In the absence of covariates it is customary to assume that the activity centers are uniformly distributed over $\mathcal{S}$, however, in the case where covariates are available that could explain the distribution of activity centers in space, we can allow for the distribution of activity centers to be non-uniform. For a discrete state-space, conditional on the total population size N, the activity center locations have a multinomial distribution with cell probabilities $\pi(s_i)$

$$\pi(s_i) \propto \frac{e^{\gamma_1 D_{1i}+\ldots\gamma_m D_{mi}}}{\sum e^{\gamma_1 D_{1i}+\ldots\gamma_m D_{mi}}}, \quad (2)$$

allowing for the distribution of individuals to be modeled as a function of covariates, **D**, thought to explain spatial variation in density. Under this formulation of the model, density within a given grid cell is obtained by allocating the population N among the cells of the landscape according to

$$E(N(s_i)) = N\frac{e^{\gamma_1 D_{1i}+\ldots\gamma_m D_{mi}}}{\sum e^{\gamma_1 D_{1i}+\ldots\gamma_m D_{mi}}}, \quad (3)$$

(Royle et al. 2014: chapter 11).

Mink activity has been positively related to densely vegetated coniferous and mixedwood shorelines with little urban development (Racey and Euler 1983), and mink distribution has been shown to be strongly correlated with density of mature tree species, saplings, and shrubs (Mason and MacDonald 1983). Based on these previous findings, we considered two density covariates: D_{cover} – percent overstory and understory vegetation, and D_{d2city} – the distance to the nearest city or town. D_{cover} was calculated as described above, but for the 200 × 200 m state-space grid cell, and D_{d2city} was computed as the distance between the center point of each 200 × 200 m state-space grid cell and the nearest town, city or village in the New York State Place Locations GIS data set. There was little variability in the size of the nine town/city/villages within the study area. Both **P** and **D** were standardized to have mean 0 and unit variance.

We formulate the model conditional on population size N for the prescribed state-space, and we estimate the parameters $\beta_{1,\ldots,m}$ and N jointly by maximum likelihood (the formulation of the model conditional on N is usually called the full likelihood in closed population capture–recapture, see Borchers et al. (2002)). A key consideration in the methods outlined above is the treatment of the activity centers s_i because they are never known in practice. We adopt an integrated likelihood approach (Borchers and Efford 2008) using a function that evaluates the likelihood of the parameters of the SCR model integrated over all possible activity centers.

One major assumption of standard SCR models is that observations of individuals are adequately described using encounter models based on Euclidean distance, i.e., $d(x_j, s_i)$ in Eq. 1 is assumed to be the usual Euclidean distance between trap locations x_j and activity center s_i

$$d_{\text{Euc}}(x_j, s_i) = \sqrt{(x_{1j} - s_{1i})^2 + (x_{2j} - s_{2j})^2}$$

However, dendritic networks are structured such that streams can be close in Euclidean space, but much farther in stream distance. For such systems, a sensible alternative to Euclidean distance for describing space use is the least-cost path distance (Beier et al. 2008, Sutherland et al. 2015). Given a discrete landscape $\mathcal{V}$, let $\mathcal{L}(v_0{:}v_t) = \{v_0, \ldots, v_t\}$ denote any path comprised of pairwise adjacent pixels connecting points v_0 and v_t. The least-cost path distance is defined by $d_{\text{lcp}}(v_0, v_t) = \min_{\mathcal{L}} \sum_{u=0}^{t} \text{cost}(v_u, v_{u+1}) \times d_{\text{Euc}}(v_u, v_{u+1})$ where d_{Euc} is the usual Euclidean distance between adjacent points of the path connecting v_0 and v_t and cost(v_u, v_{u+1}) is the cost of moving from v_u to v_{u+1}. We define the cost function by $\log(\text{cost}(v_u, v_{u+1})) = \alpha_2 \frac{z(v_u)+z(v_{u+1})}{2}$ where z is any covariate defined for all cells of the discrete landscape. With this cost function if $\alpha_2 = 0$ then least-cost path distance reduces to ordinary Euclidean distance. Either distance metric, d_{Euc} or d_{lcp} may be used in the formulation of the SCR likelihood thus yielding an explicit estimate of the cost parameter α_2 and therefore an explicit model of connectivity, as defined by least-cost path.

The ecological distance model requires estimating a single additional parameter, α_2, that quantifies the strength of association between a species and a particular landscape covariate. In the case of American mink, we generated a distance to water surface and calculated the distance from the centroid of each grid cell to the nearest stream (Sutherland et al. 2015). For example, in the context of mink in stream networks, when $\alpha_2 = 0$, there

is no landscape resistance and movement is exactly Euclidean, and as α_2 increases, mink activity is more associated with water and movement is more likely along the waterway than away from it (see Sutherland et al. 2015). In Fig. 2, we illustrate how the cost parameter (α_2) can be estimated when sampling occurs only along water within a stream network setting. The branching pattern of stream networks allows us to sample streams that are close in Euclidean space. This generates a spatial pattern of observations that, if a deviation from Euclidean-based expectations is observed, provides information about apparent costs associated with the landscape structure of interest. In order to account for the riparian nature of American mink, we fitted and compared both the Euclidean distance SCR model and the ecological distance SCR model. Further, we estimated potential landscape connectivity using the maximum likelihood estimates of the movement parameter, σ, and the cost parameter, α_2, and computed cell specific connectivity $C_s = \sum_{i \neq j} \exp(-\hat{\alpha}_1 \times d_{\text{lcp}}[s_i,s])$, that measures how connected each pixel on the landscape is to all other pixels on the landscape. The values, and the resulting surface, is scaled to represent relative connectivity values on the scale 0–1 (i.e., C_s/ max (C_s)).

In total we fitted 64 competing models that included the null model (no covariates or sex effects) and all combinations of encounter ($n = 1$) and density ($n = 2$) covariates and sex effects ($n = 4$; sex-specific σ only, sex-specific baseline detection only, both σ and detection varying by sex, or no sex effects), and for each combination, we fitted both the Euclidean distance model (Euc) and the ecological distance model (Ecol).

Functions for computing the likelihood and obtaining the maximum likelihood estimates (MLEs) were written in the R language (R Development Core Team 2013). The models were fitted using nlm to minimize the integrated likelihood function with the code provided in (Sutherland et al. 2015). We calculated AIC_c values for each model and used their differences (ΔAIC_c) to rank candidate models, where the model with the lowest AIC_c is the model with the highest predictive performance in the model set. Model averaged parameter estimates and model averaged predicted density surfaces were calculated using model weights based on AIC_c values.

Results

Genetic results

DNA was extracted from 206 scat specimens. Of these, 71 (34.5%) did not yield sufficient DNA quality/quantity based on the initial four-locus test. Based on microsatellite and COI data, six specimens with good DNA were determined to be non-mink and 116 specimens had a sufficient number of genotyped loci to analyze (58% of mink specimens). Of these, we successfully genotyped all 12 microsatellite loci in 73 specimens, 11 loci in 21 specimens, 10 loci in eight specimens, and three to six loci were missing in 14 additional specimens. The average genotypic mismatch rate per replicate per locus was 10.4%± 0.044 (SD), with estimates ranging from 4.5% to 17.1% across loci. Resolving two types of genotyping error (based on a consensus genotype deduced from the first two replicates and requiring only one observation of an alternate allele to call a heterozygote), average allelic dropout rate was estimated as 21.4% per replicate per heterozygous locus (range 9–40%) and false allele rate was 2.4% per replicate per genotyped specimen (range 0.6–4.4% among loci).

Unbiased PID, including the sex marker, was 8.65×10^{-10} among unrelated individuals and PID(sib) was 2.93×10^{-04}. The three genotypes containing only six loci (i.e., worse case) all had probability of being drawn from the population $<3.89 \times 10^{-07}$, so they are not likely to match other genotypes by chance.

Based on three replicate runs of SHAZA using a mismatch rate of 10%, the 116 multilocus genotypes resulted in 34 inferred individuals (13 female, 12 male, nine unknown). These analyses are based on genotypes with zero to two or occasionally three locus mismatches out of 12 loci, and likelihood ratio tests allowing cumulative type I error of no more than 0.50 false recaptures.

We generated individual-by-trap encounter histories based on the locations at which an individuals scat was found (i.e., by allocating them to the closest trap; see Materials and methods: Study design and mink scat collection), which resulted in 19 mink being detected at a single trap and 15 mink that were trapped multiple times, including two to five recaptures per individual (Table 1). Two individuals were observed in more than one stream transect, with distances moved of 1.31 and 1.45 km.

SCR results

Based on AIC_c, in general, the ecological distance models were better supported than their Euclidean distance model counterparts (Table 2). Abundance estimates under the Euclidean distance models were systematically lower than ecological distance models (Table 2), consistent with the notion that unmodeled heterogeneity in capture probability results in negatively biased estimates of population size (Sutherland et al. 2015). Because of the clear support, from here we present the results from the preferred ecological distance model only (Table 3).

Models that included covariate effects on density were more parsimonious than the null model with no

Table 1. Summary of the frequency of (re)captures.

No. encounters	1	2	3	4	5
Frequency	19	4	8	2	1

Notes: There were a total of 34 unique individuals caught, 15 of which were detected more than once (i.e. scat found at >1 trap) and 2 were detected at more than one stream transect. Unique trap data (Binomial encounters) are used in the analysis.

TABLE 2. A total of 32 competing models were fitted in order to include all combinations of covariates for encounter probability (n = 1; cover = percent cover of trees and shrubs) and density (n = 2; cover and d2city = distance to nearest town, city, or village center), and sex effect (n = 4; intercept, σ, both intercept and σ, or no sex effect) as well as including no covariate models (null).

				AIC_c			N		Ecological distance		
Encounter	Density	Sex effect	n Par	Ecol	Euc	ΔAIC_c	Ecol	Euc	ΔAIC_c	Weight	Cost
1	d2city	Intercept	6 (5)	508.25	510.46	2.21	895.52	779.70	0.00	0.47	3.77
1	d2city	Both	7 (8)	510.08	510.80	0.72	849.37	721.68	1.83	0.19	3.71
1	cover + d2city	Intercept	7 (8)	511.56	511.37	−0.19	885.83	743.73	3.31	0.09	3.71
cover	d2city	Intercept	7 (8)	511.62	513.38	1.76	898.27	782.80	3.37	0.09	3.74
1	cover + d2city	Both	8 (9)	513.09	511.89	−1.20	822.97	683.46	4.84	0.04	3.74
cover	d2city	Both	8 (9)	513.72	513.93	0.21	859.53	726.15	5.47	0.03	3.71
1	d2city	None	5 (4)	514.23	516.21	1.98	793.73	661.50	5.98	0.02	3.92
cover	cover + d2city	Intercept	8 (9)	515.28	514.82	−0.46	889.47	744.98	7.03	0.01	3.72
1	cover + d2city	None	6 (5)	515.49	515.71	0.22	957.65	665.49	7.24	0.01	4.26
cover	cover + d2city	Both	9 (10)	517.16	515.62	−1.54	823.39	681.12	8.91	0.01	3.73
1	1	Intercept	5 (4)	517.20	520.61	3.41	465.34	397.77	8.95	0.01	3.84
1	d2city	σ	6 (5)	517.42	519.16	1.74	801.21	663.23	9.17		3.98
cover	d2city	None	6 (5)	517.43	519.13	1.70	793.84	664.60	9.18	0.00	3.92
cover	cover + d2city	None	7 (8)	518.31	518.84	0.53	1005.63	671.32	10.06	0.00	4.50
1	cover + d2city	σ	7 (8)	518.48	518.87	0.39	1029.60	665.65	10.23	0.00	5.54
1	1	Both	6 (5)	519.00	521.08	2.08	438.90	366.96	10.75	0.00	3.92
1	cover	Both	7 (8)	520.09	521.38	1.29	916.95	696.76	11.84	0.00	5.48
1	cover	Intercept	6 (5)	520.24	521.21	0.97	424.48	678.97	11.99	0.00	3.99
cover	1	Intercept	6 (5)	520.40	523.51	3.11	465.56	395.20	12.15	0.00	3.84
cover	d2city	σ	7 (8)	520.87	522.31	1.44	801.15	666.40	12.62	0.00	3.98
cover	cover + d2city	σ	8 (9)	521.40	522.24	0.84	1061.35	672.54	13.15	0.00	5.58
1	cover	None	5 (4)	521.59	525.99	4.40	905.46	617.09	13.34	0.00	4.57
cover	1	Both	7 (8)	522.45	524.19	1.74	438.92	364.72	14.20	0.00	3.92
cover	cover	Both	8 (9)	523.35	524.81	1.46	947.58	692.06	15.10	0.00	5.48
cover	cover	Intercept	7 (8)	523.66	524.02	0.36	415.70	718.12	15.41	0.00	3.99
cover	cover	None	6 (5)	523.73	528.25	4.52	968.70	647.46	15.48	0.00	5.13
1	1	None	4 (3)	523.73	527.20	3.47	410.50	334.86	15.49	0.00	4.10
1	cover	σ	6 (5)	524.34	528.58	4.24	944.45	607.10	16.09	0.00	5.53
cover	cover	σ	7 (8)	526.59	531.10	4.51	983.60	636.13	18.34	0.00	5.54
cover	1	None	5 (4)	526.60	529.96	3.36	412.01	334.82	18.35	0.00	4.23
1	1	σ	5 (4)	526.70	529.96	3.26	410.86	334.86	18.45	0.00	4.10
cover	1	σ	6 (5)	529.80	532.93	3.13	412.43	334.82	21.55	0.00	4.23

Notes: In addition to the standard SCR model in which movement is assumed to be Euclidean (Euc), we fitted the same 32 competing models using the Ecological Distance model (Ecol) to explicitly estimate the association of mink to water (Ecol, cost or resistance parameter is α_2). We estimated abundance under each model and calculated and compared models using AIC_c values and their differences (ΔAIC_c).

covariates ($\Delta AIC_{\text{null-best}}$ = 15.48; Table 2). Two models within two AIC units of each other had a cumulative weight of 0.66. Neither of the top two models included the covariate percent of trees and shrubs on encounter probability (Table 4). There was support for sex specific detection ($p_{0,\text{sex}}$) and movement (σ_{sex}) parameters, and an effect of distance to city, town, or village center (d2city) on mink density; the cumulative weight of all models containing the covariate d2city was 0.99 (Table 2). The sex-specific estimates of the movement scale parameter σ_{sex} were σ_{male} = 1.01 km (95% CI = 0.74–2.71) and σ_{female} = 0.82 km (95% CI = 0.67–1.19). Sex-specific estimates of the baseline encounter probability, $p_{0,\text{sex}}$, were $p_{0,\text{male}}$ = 0.07 (95% CI = 0.04–0.12) and $p_{0,\text{female}}$ = 0.38 (95% CI = 0.27–0.49). The best supported model suggests that mink density is influenced by the distance to city/town/village centers, with a model averaged β_{d2city} = 0.90 (95% CI = 0.33–1.46) (Table 4). Specifically, the expected mink density per grid cell increases with increasing distance from city/town/village centers.

Because the distances to the nearest city/town/village center are known for each grid cell in $\boldsymbol{S}$, parameter estimates can be used to predict where mink are most (and least) likely to occur and, multiplying estimated multinomial cell probabilities by $\hat{N}$, we can estimate the expected number of mink in each grid cell $\hat{N}(s) = \hat{N}\hat{\pi}(s)$; Fig. 3). Moreover, we have the ability to estimate absolute density because of the explicit consideration of a prescribed state space in the SCR model. Our study area of interest consisted of 9702 pixels of area 200 × 200 m (i.e., 388.08 km^2),

TABLE 3. Maximum likelihood estimates (MLE) with associated standard errors (SE) and a description of the parameter in the spatial capture–recapture model.

Parameter	Description	Estimate	SE	Transformation (95% CI)
$\alpha_{0,female}$	intercept of the female encounter model	−0.49	0.22	logit: $p_{0,f} = 0.38$ (0.27–0.49)
$\alpha_{0,male}$	intercept of the male encounter model	−2.58	0.30	logit: $p_{0,m} = 0.07$ (0.04–0.12)
$\alpha_{1,female}$	scale parameter (km) of the female bivariate normal encounter model	0.73	0.19	$\sqrt{\frac{1}{2\times\alpha_1}}$: $\sigma = 0.82$ (0.67–1.19)
$\alpha_{1,male}$	scale parameter (km) of the male bivariate normal encounter model	0.49	0.21	$\sqrt{\frac{1}{2\times\alpha_1}}$: $\sigma = 1.01$ (0.74–2.71)
$log(n_0)$	estimated number of unobserved mink	6.73	0.24	log: 838.62 (523.67–1342.99)
α_2	resistance or cost parameter measuring association with water	1.33	0.40	log: 3.78 (1.73–8.22)
ϕ_{male}	probability of being a male	0.59	0.35	logit: 0.64 (0.46–0.79)

Notes: Here we present model averaged estimates for parameters n_0, α_0, α_1, α_2, and ψ_{sex} as they are present in all models. The transformation depicts values in the original scale.

with an estimated total population size of 873. Following Royle et al. (2014), we estimated the proportion of the population that is male, ϕ_{male}, which allows for the reporting of sex-specific abundance and density; $N_{male} = \phi_{male}\hat{N} = 559$ (95% CI = 357–881) and $N_{female} = \hat{N}_{female} = \hat{N} - \hat{N}_{male} = 314$ (95% CI = 201–496). Density is computed by dividing by area: $\hat{D}_{male}$ = 1.44/km^2 (95% CI = 0.92–2.27/km^2), $\hat{D}_{female}$ = 0.81/km^2 (95% CI = 0.52–1.28/km^2). To account for model selection uncertainty, we present a model averaged estimate of total density for the entire study area and model averaged density surface, i.e., the sum of the estimated per pixel density weighted by the AICc model weight (Fig. 3). The overall predicted density ($D = \frac{1}{A}\sum_{s\in S}\hat{D}(s)$, where $\hat{D}(s)$ is the estimated per pixel population size and A is the area of the state space) was 2.25 mink/km^2. We used distance to nearest city/town/village center as a covariate and note that, particularly in the northeast part of the state space (Fig. 3), distances are greater than those within the range of the data (calculated as the maximum distance to city value within $2\hat{\sigma}_{male}$ km of any trap). Therefore, we provide a conservative estimate of density that we adjusted to consider only the cells of the state space that were within the effective range of our data. The adjusted study area consisted of 9159 pixels of area 200 × 200 m (i.e. 366.36 km^2). This translates to a conservative density estimate of 1.37 mink/km^2 within the reduced area of interest.

Finally, application of the ecological distance model provides an estimated cost (α_2) of movement away from water which was $\hat{\alpha_2} = 3.78$. This cost parameter is a direct

TABLE 4. Model specific point estimates (MLEs) of the covariate coefficients (cover = percent cover of trees and shrubs; d2city = distance to nearest town, city, or village center).

Encounter model (P)	Density model (D)	Sex model	Pcover	Dd2city	Dcover
1	1	both	–	–	–
1	1	intercept	–	–	–
1	1	n	–	–	–
1	1	σ	–	–	–
1	d2city	both	–	0.92	–
1	d2city	intercept	–	0.91	–
1	d2city	n	–	0.93	–
1	d2city	σ	–	0.93	–
1	cover	both	–	–	−4.37
1	cover	intercept	–	–	0.33
1	cover	n	–	–	−5.08
1	cover	σ	–	–	−5.58
1	cover + d2city	both	–	0.91	−0.6
1	cover + d2city	intercept	–	0.91	−0.22
1	cover + d2city	n	–	0.74	−3.61
1	cover + d2city	σ	–	0.72	−4.36
cover	1	both	0	–	–
cover	1	intercept	0.01	–	–
cover	1	n	0.05	–	–
cover	1	σ	0.05	–	–
cover	d2city	both	−0.06	0.93	–
cover	d2city	intercept	−0.05	0.92	–
cover	d2city	n	0	0.93	–
cover	d2city	σ	0	0.93	–
cover	cover	both	0.13	–	−4.44
cover	cover	intercept	−0.04	–	0.4
cover	cover	n	0.21	–	−5.58
cover	cover	σ	0.23	–	−5.71
cover	cover + d2city	both	−0.01	0.91	−0.58
cover	cover + d2city	intercept	−0.03	0.92	−0.18
cover	cover + d2city	n	0.16	0.71	−4.02
cover	cover + d2city	σ	0.19	0.7	−4.6
		support	0.15	0.99	0.18

Notes: By definition, competing models did not contain all covariate effects, so we present estimated covariate coefficients ($\beta_{d,c}$ and $\beta_{p,c}$) from all models. We provide the support for each covariate, based on the accumulated weight of all models containing that covariate. The sex model includes intercept, σ, and both intercept and σ.

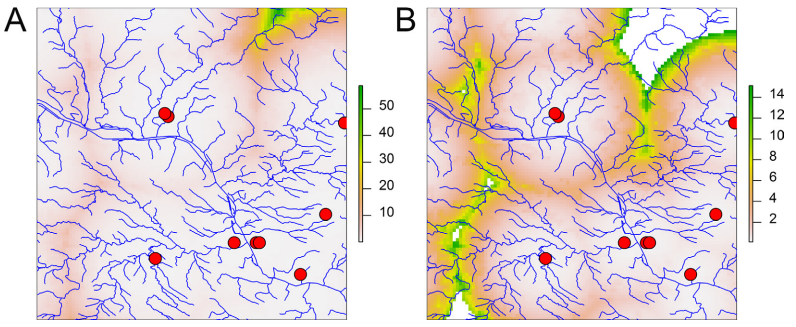

FIG. 3. Using the maximum likelihood estimates of the parameters, the expected density of mink can be computed for each 200 m × 200 m grid cell. We present a model averaged predicted density surface, i.e. the sum of the estimated per pixel density weighted by the AICc model weight, expressed as an expected density map for the state-space S of the spatial capture-recapture model. (A) represents the expected mink density per km^2 (2.25 mink/km^2) within the entire state-space (388 km^2) and (B) represents expected mink density (1.37 mink/km^2) adjusted to consider only the cells within the state-space that were within the effective range of our data (366 km^2). Red dots in A and B represent town/village/city centers.

measure of the affinity of mink to streams and allows for the calculation of relative frequency of use of specific parts of the landscape (Sutherland et al. 2015). For example, and following Sutherland et al. (2015: Relative frequency of use), based on our estimates of α_1 and α_2, mink utilize areas 0.5 km along the stream 1.99 times (male) to 2.84 times (female) more frequently than the same distance away from the stream. We computed the potential connectivity across the study area (Fig. 4), demonstrating that despite branches of streams not being physically connected, landscape connectivity can be maintained between branches by movement between close proximity but distinct stream sections.

DISCUSSION

This study simultaneously estimated density and landscape connectivity from individual encounter history data. Specifically, we demonstrated an application of using capture–recapture to develop a model of animal density using a least-cost path model for individual encounter probability that accounts for non-Euclidean connectivity of a highly structured landscape (i.e., riparian network). Many studies strive to either estimate abundance of animal populations or to model landscape connectivity, but we are unaware of any studies that have simultaneously modeled abundance while accounting for connectivity of a landscape.

We used the explicit least-cost path model of connectivity as a better model for encounter probability of individuals in a capture–recapture study. A by-product of our approach, which may be of direct interest in many studies of landscape connectivity, is a direct or data-based estimate of the resistance parameter α_2, which is directly related to the connectivity of the landscape as a function of distance from water or any other covariate of interest (Sutherland et al. 2015). Estimating landscape resistance to movement is often the basis for landscape connectivity modeling and corridor design applications, but the most common approach to estimating values for resistance surfaces is by using expert opinion (Zeller et al. 2012). The model we present obviates the need for using expert opinion to derive resistance to movement values, and instead we estimate resistance directly by use of our encounter model.

Stream networks or other forms of dendritic geometries can constrain animal movement (Grant et al. 2009, 2010), and our model allowed us to describe this movement associated with the species–landscape interaction. Mink in our study were associated with stream networks; given a particular location on a stream, mink were predicted to use locations 0.5 km along the water 1.99 times more frequently for males and 2.84 times more frequently for females than 0.5 km away from the water.

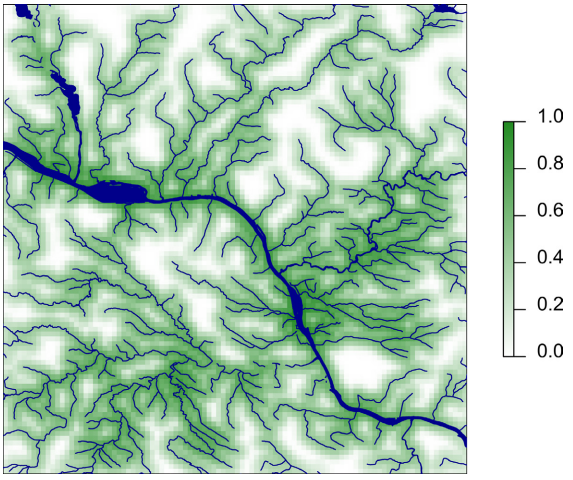

FIG. 4. The connectivity surface of the study area based on estimated parameters from the ecological distance model described in the text. Using the maximum likelihood estimates of the movement parameter, σ, and the cost parameter, α_2, we computed cell specific connectivity that measures, $C_s = \sum_{i \neq j} \exp(-\hat{\alpha}_1 \times d_{\text{lcp}}[s_i, s_j])$, how connected each pixel on the landscape is to all other pixels on the landscape. The values, and the resulting surface, is scaled to represent relative connectivity values on the scale 0 to 1 (i.e., $C_s/\max(C_s)$).

Although poorly documented in the United States, mink are reported to be associated with vegetated areas adjacent to water (Dunstone 1993), and have been found to be negatively associated with urbanization (Lundy and Montgomery 2010, Wolff et al. 2015), human activity (Melero et al. 2008), and development (Racey and Euler 1983). Our findings are in agreement; in our study, mink densities were higher in areas farther from urban centers, and mink activity was positively associated with water. In Canada, mink activity was documented to be lower around lakes with cottage development (Racey and Euler 1983), but the specific effects of increased urbanization on mink is unclear (Gehrt et al. 2010). The incorporation of auxiliary data (covariates) to explain the spatial distribution and space use of individuals provided results that are biologically intuitive and interpretable given what is know about the ecology of American mink (Dunstone 1993).

We note that SCR models do not require that individuals are scatting randomly on the landscape, just that the distribution of scats is described by the specified encounter probability model. One of the models we considered posits that the probability of scat deposition at some point X is a nonlinear cost-weighted function of distance from activity center S. We compared this model to a model which posits that scat deposition is a monotone decreasing function of Euclidean distance. If we had other models for how scat distribution is concentrated around a mink's activity center, then we could fit such models and compare them with ours, but explicit information to suggest specific alternative models of scat deposition is lacking. One other approach to investigating whether scat deposition is not random with respect to home range usage would be to obtain a data set with home ranges estimated from telemetry and observe the distribution of scats relative to an estimated home range. But as far as we know, such data have not been collected, nor has this issue received attention in the literature. Thus, plausible models beyond Euclidean distance and our new model of distance-from-stream based connectivity are not evident. No matter the relevance of our specific models to scatting behavior, the effect of misspecifying the model is unclear, although considerable existing simulation work suggests a fair amount of robustness to misspecification of encounter probability models (Efford and Mowat 2014, Royle et al. 2015, Sutherland et al. 2015).

In summary, we demonstrated the application of a spatially explicit model of density, accounting for heterogeneity in spatial distribution of individuals resulting from species-specific space usage and heterogeneous encounter probabilities induced by landscape structure. The ability to estimate landscape connectivity directly from capture–recapture data represents a large conceptual advance and has implications for conservation. Indeed, landscape connectivity has relevance for long-term persistence of species and has gained increased importance as landscapes become more fragmented (Lindenmayer et al. 2008). The ability to quantify the specific cost of movement associated with any feature of the landscape has great utility for use in conservation and management applications for a wide suite of species, and has important implications for considering landscape connectivity, and would help inform corridor design work.

Acknowledgments

The authors thank three anonymous reviewers for comments on a draft of this manuscript. We are thankful to Harmony Borchardt-Wier for assistance with genetic analyses. We thank the many landowners who allowed us access to their lands to search for mink scats and to Conservation Canines for employing their highly efficient dogs. Part of this research was performed using the ATLAS HPC Cluster, a compute cluster with 672 cores, 4 Tesla M2090 GPU accelerators, supported by NSF grants (Award #1059284 and #0832782). This work was supported by the New York State Department of Environmental Conservation and the Hudson River Natural Resource Trustees. The conclusions and opinions presented here are those of the authors and the U.S. Geological Survey and do not represent the official position of the New York State Department of Environmental Conservation, or the Hudson River Natural Resource Trustees. Any use of trade, firm, or product names is for descriptive purposes only and does not imply endorsement by the U.S. Government.

Literature Cited

Basu, N., A. Scheuhammer, S. Bursian, J. Elliot, K. Rouvinen-Watt, and H. Chan. 2007. Mink as a sentinel species in environmental health. Environmental Research 103:130–144.

Beier, P., D. Majka, and W. Spencer. 2008. Forks in the road: choices in procedures for designing wildland linkages. Conservation Biology 22:836–851.

Bonesi, L., and D. Macdonald. 2004. Differential habitat use promotes sustainable coexistence between the specialist otter and the generalist mink. Oikos 3:509–519.

Borchers, D. L., and M. G. Efford. 2008. Spatially explicit maximum likelihood methods for capture–recapture studies. Biometrics 64:377–385.

Borchers, D., S. Buckland, and W. Zucchini. 2002. Estimating animal abundance: closed populations. Springer, London, UK.

Burgess, S., and J. Bider. 1980. Effects of stream habitat improvements on invertebrates, trout populations, and mink activity. Journal of Wildlife Management 44:871–880.

Dunstone, N. 1993. The mink. T. & A.D. Poyser, Calton, Staffordshire, UK.

Efford, M., and G. Mowat. 2014. Compensatory heterogeneity in spatially explicit capture–recapture data. Ecology 95: 1341–1348.

Efford, M. G., D. K. Dawson, and D. L. Borchers. 2009. Population density estimated from locations of individuals on a passive detector array. Ecology 90:2676–2682.

Enders, R. K. 1952. Reproduction in the mink *(Mustela vison)*. Proceedings of the American Philosophical Society 96: 691–755.

Erb, J., M. S. Boyce, and N. C. Stenseth. 2001. Spatial variation in mink and muskrat interactions in Canada. Oikos 93:365–375.

Fagan, W. F. 2002. Connectivity, fragmentation, and extinction risk in dendritic metapopulations. Ecology 83:3243–3249.

Gehrt, S. D., S. P. D. Riley, and B. L. Cypher, editors. 2010. Urban carnivores: ecology, conflict, and conservation. Johns Hopkins University Press, Baltimore, Maryland, USA.

Gerell, R. 1970. Home ranges and movements of the mink *Mustela vison* in southern Sweden. Oikos 21:160–173.

Grant, E. H. C., L. E. Green, and W. H. Lowe. 2009. Salamander occupancy in headwater stream networks. Freshwater Biology 54:1370–1378.

Grant, E., J. Nichols, W. Lowe, and W. Fagan. 2010. Use of multiple dispersal pathways facilitates amphibian persistence in stream networks. Proceedings of the National Academy of Sciences USA 107:6936–6940.

Haydon, D. T., N. C. Stenseth, M. S. Boyce, and P. E. Greenwood. 2001. Phase coupling and synchrony in the spatiotemporal dynamics of muskrat and mink populations across Canada. Proceedings of the National Academy of Sciences USA 98:13149–13154.

Lampa, S., K. Henle, R. Klenke, M. Hoehn, and B. Gruber. 2013. How to overcome genotyping errors in non-invasive genetic mark–recapture population size estimation: a review of available methods illustrated by a case study. Journal of Wildlife Management 77:1490–1511.

Lindenmayer, D. B., et al. 2008. A checklist for ecological management of landscapes for conservation. Ecology Letters 11:78–91.

Loukmas, J., and R. Halbrook. 2001. A test of the mink habitat suitability index model for riverine systems. Wildlife Society Bulletin 29:821–826.

Lundy, M., and W. Montgomery. 2010. A multi-scale analysis of the habitat associations of European otter and American mink and the implications for farm scale conservation schemes. Biodiversity & Conservation 19:3849–3859.

Macbeth, G. M., D. Broderick, J. R. Ovenden, and R. C. Buckworth. 2011. Likelihood-based genetic mark–recapture estimates when genotype samples are incomplete and contain typing errors. Theoretical Population Biology 80:185–196.

Marshall, W. 1936. A study of the winter activities of the mink. Journal of Mammalogy 17:382–392.

Mason, C., and S. MacDonald. 1983. Some factors influencing the distribution of Mink *(Mustela vison)*. Journal of the Zoological Society of London 200:281–302.

Melero, Y., S. Palazón, E. Revilla, J. Martelo, and J. Gosàlbez. 2008. Space use and habitat preferences of the invasive American mink *(Mustela vison)* in a Mediterranean area. European Journal of Wildlife Research 54:609–617.

Niemimma, J. 1955. Activity patterns and home ranges of the American mink *Mustela vison* in the Finnish outer archipelago. Acta Zoologica Fennica 32:117–121.

Pompanon, F., A. Bonin, E. Bellemain, and P. Taberlet. 2005. Genotyping errors: causes, consequences and solutions. Nature Reviews Genetics 6:847–859.

R Development Core Team. 2013. R: a language and environment for statistical computing. R Foundation for Statistical Computing, Vienna, Austria. http://www.R-project.org

Racey, G., and D. Euler. 1983. Changes in mink habitat and food selection as influenced by cottage development in central Ontario. Journal of Applied Ecology 20:387–401.

Reed, S. E., A. L. Bidlack, A. Hurt, and W. M. Getz. 2011. Detection distance and environmental factors in conservation detection dog surveys. Journal of Wildlife Management 75:243–251.

Rousset, F. 2008. Genepop'007: a complete reimplementation of the Genepop software for Windows and Linux8. Molecular Ecology Resources 8:103–106.

Royle, J. A., R. B. Chandler, K. Gazenski, and T. Graves. 2013a. Spatial capture–recapture models for jointly estimating population density and landscape connectivity. Ecology 94:287–294.

Royle, J. A., R. B. Chandler, C. C. Sun, and A. K. Fuller. 2013b. Integrating resource selection information with spatial capture–recapture. Methods in Ecology and Evolution 4:520–530.

Royle, J. A., R. B. Chandler, R. Sollmann, and B. Gardner. 2014. Spatial capture–recapture. Elsevier, Oxford, UK.

Royle, J. A., C. Sutherland, A. K. Fuller, and C. C. Sun. 2015. Likelihood analysis of spatial capture–recapture models for stratified or class structured populations. Ecosphere 6:22.

Ruibal, M., R. Peakall, A. Claridge, and K. Firestone. 2009. Field-based evaluation of scat DNA methods to estimate population abundance of the spotted-taled quoll *(Dasyurus maculatus)*, a rare Australian marsupial. Wildlife Research 36:721–736.

Shier, C., and M. S. Boyce. 2009. Mink prey diversity correlates with mink-muskrat dynamics. Journal of Mammalogy 90:897–905.

Shimatani, Y., T. Takeshita, S. Tatsuzawa, T. Ikeda, and R. Masuda. 2010. Sex determination and individual identification of American minks *(Neovison vison)* on Hokkaido, northern Japan, by fecal DNA analysis. Zoological Science 27:243–247.

Sollmann, R., B. Gardner, and J. L. Belant. 2012. How does spatial study design influence density estimates from spatial capture–recapture models? PLoS ONE 7:e34575.

Sutherland, C., A. K. Fuller, and J. Royle. 2015. Modelling non-Euclidean movement and landscape connectivity in highly structured ecological networks. Methods in Ecology and Evolution 6:169–177.

Valière, N. 2002. GIMLET: a computer program for analysing genetic individual identification data. Molecular Ecology Notes 2:377–379.

Waits, L. P., G. Luikart, and P. Taberlet. 2001. Estimating the probability of identity among genotypes in natural populations: cautions and guidelines. Molecular Ecology 10:249–256.

Williams, B. K., J. D. Nichols, and M. J. Conroy. 2002. Analysis and management of animal populations: modeling, estimation and decision making. Academic Press, Cambridge, UK.

Wolff, P., C. A. Taylor, E. J. Heske, and R. L. Schooley. 2015. Habitat selection by American mink during summer is related to hotspots of crayfish prey. Wildlife Biology 21:9–17.

Yamaguchi, N., S. Rushton, and D. W. Macdonald. 2003. Habitat preferences of feral American mink in the Upper Thames. Journal of Mammalogy 84:1356–1373.

Zeller, K. A., K. McGarigal, and A. R. Whiteley. 2012. Estimating landscape resistance to movement: a review. Landscape Ecology 27:777–797.

Supporting Information

Additional supporting information may be found in the online version of this article at http://onlinelibrary.wiley.com/doi/10.1890/15-0315.1/suppinfo

Data Availability

Data associated with this paper have been deposited in Dryad: http://dx.doi.org/10.5061/dryad.s7ph4.